INTERNATIONAL TURBULENCE COMPARISON EXPERIMENT (ITCE-81)

L. R. TSVANG, S. L. ZUBKOVSKII, B. A. KADER, M. A. KALLISTRATOVA
Institute of Atmospheric Physics of the U.S.S.R. Academy of Sciences, U.S.S.R.

T. FOKEN, V. GERSTMANN
Meteorological Main Observatory of the Meteorological Service of the G.D.R., Potsdam, G.D.R.

A. PRZADKA
Institute of Engineering Problems of the Warsaw Polytechnical Institute, Poland

Ya. PRETEL, Ya. ZELENY
Institute of Atmospheric Physics of the Czechoslovak Academy of Sciences, Czechoslovakia
and
J. KEDER
Hydrometeorological Institute, Czechoslovakia

(Received in final form 22 June, 1984)

Abstract. The main results of the International Turbulence Comparison Experiment (Tsimlyansk, U.S.S.R., June–July 1981) are presented. Groups from G.D.R., Poland, U.S.S.R., and Czechoslovakia took part in the experiment, while Bulgarian researchers were present as observers. A comparison of in situ measurements (by acoustic anemometers, thermoanemometers, and resistance thermometers) among themselves and with remote soundings (by sodars) was made. Simultaneous measurements of turbulent fluctuation characteristics and of wind velocity and temperature profiles were performed by different instruments. The results and temperature profiles were performed by different instruments. The results of these measurements were used to estimate the comparative accuracy of various models proposed for the evaluation of turbulent fluxes from profile data.

1. Introduction

In recent years, investigations related to the World Climate Program have aroused more and more interest. The problem of quantitative description of the atmosphere-surface interaction is one of the more important parts of the program. It is known that the interaction of the atmosphere with the underlying surface is determined by the vertical transfers of momentum, heat and humidity. Many instruments have been designed in many countries to measure turbulent fluctuations in the atmospheric surface layer, in order to determine the turbulent fluxes by the eddy correlation method. However, many questions related to these measurements are not yet answered. There is no standard method of fluctuation measurements which is universally considered to be the best. Therefore the comparison of results obtained using different instruments is necessary

Boundary-Layer Meteorology **31** (1985) 325–348. 0006–8314/85.15

to help identify problems with the instruments. For this purpose, several international experiments on turbulence measurement comparisons have been carried out in recent years (see Businger *et al.*, 1967; Miyake *et al.*, 1971; Tsvang *et al.*, 1973; Dyer *et al.*, 1982). The results of these comparisons have made it possible to reveal and to eliminate some defects in the instruments used by different groups of researchers. Between June 16 and July 30, 1981, another international turbulence comparison experiment (ITCE-81) was carried out at the Tsimlyansk field station (in the Rostov region, U.S.S.R.) of the Institute of Physics of the Atmosphere (IPA) of the U.S.S.R. Academy of Sciences. Besides IPA, scientists from the Meteorological Main Observatory (MMO) in Potsdam of the G.D.R. Meteorological Service, Institute of Engineering Problems of the Warsaw Polytechnical Institute (WPI, Poland), Institute of Physics of the Atmosphere of the Czechoslovak Academy of Sciences (IPACz) in Prague, Hydrometeorological Institute (HMI) of the Ministry of Forestry and Water Resources (Czechoslovakia) took part. Two scientists from the Institute of Hydrology and Meteorology of the Bulgarian Academy of Sciences and from the Sofia University (Bulgaria) participated as observers.

The main purposes of the experiment were:

(1) Comparison of different turbulence measuring instruments and devices for data treatment.

(2) Estimation of the accuracy of various models suggested by different authors for the evaluation of turbulent fluxes from the data on wind velocity and temperature profiles.

2. Measuring Apparatus

The list of the used instruments, their brief description and main characteristics are given in Table I.

3. Site and Conditions of the Experiment

All measurements were taken at IPA's Tsimlyansk scientific station in the southern steppe part of the European territory of the U.S.S.R. The experimental site is a relatively homogeneous area (700 × 750 m) of uncultivated steppe (Figure 1). Laboratory facilities, habitable premises and tents for the participants are situated in the south-east corner of the site (200 × 40 m) planted with trees and shrubs. The measuring equipment was placed in two houses (see 3 in Figure 1) at a distance approximately 70–80 m from the anemometer and thermometer sensors and sodar antennae (see 4 and 5 in Figure 1). At the location of the sensors, the upwind fetch is more than 2 km for northwest, north, and northeast winds (the ground cover outside the experimental site is similar to that of the site itself). To the east, a narrow band of forest is situated at 1.4 km from the border of the site. The site has a slight slope of about 0.01 in the west direction. All measurements analysed in this paper were taken in north and northeast winds, for which the fetch is greatest. (Note that the north and northeast wind directions correspond to the maximum in the local 'wind rose'.)

TABLE I

Instruments used in ITCE-81

Measured parameters (1)	Type of the instrument (2)	Engineering characteristics (3)	Group (4)	Remarks (5)
wind velocity and temperature fluctuations u', v', w', and T'	acoustic anemometer-thermometer Kaijo Denki PAT 311	measurement range: u: 0–3 m s^{-1} or 0–30 m s^{-1} w: 0–1 m s^{-1} or 0–10 m s^{-1}	MMO, G.D.R.	u' and v' fluctuations are calculated from the measured values of two wind velocity components along the directions forming 120° angle
fluctuations u' and w'	IPA acoustic anemometer	measurement range: u': ±4.6 m s^{-1} w': ±4 m s^{-1}	IPA, U.S.S.R.	the sensor is directed along the mean wind at the beginning of each measurement run
fluctuations u'	constant temperature thermo-anemometer H-190	measurement range: u': ±5 m s^{-1}	WPI, Poland	the sensor is tied to a vane; there is also an additional temperature sensor which permits one to compensate T' fluctuations
fluctuations u', v', and w' and the total wind velocity vector u	three-component propeller anemometer W-173A	range of u measurements: 0.3–50 m s^{-1}; wind free path 30 cm	IPACz	
fluctuations T'	resistance thermometer with a 20 μm platinum wire sensor	time constant $\tau \leq 10^{-2}$ s sensitivity from 0.1 °C v^{-1} to 1 °C v^{-1}	MMO, G.D.R.	
fluctuations T'	resistance thermometer with a 10 μm tangsten wire sensor	sensitivity from 0.07 °C v^{-1} to 0.6 °C v^{-1}	IPA, U.S.S.R.	
profiles of mean wind velocity $u(z)$	monostatic sodar	carrier frequency 2000 Hz, acoustic power 6 W, sounding height 360 m, vertical resolving ability 12 m	IPA, U.S.S.R.	antenna axis is directed at 45° to horizon; longitudinal and lateral wind velocity components are measured in turn; real-time treatment of the data is carried out by a system including microcomputer D-3-28

Table I (continued)

Measured parameters (1)	Type of the instrument (2)	Engineering characteristics (3)	Group (4)	Remarks (5)
heights of the upper and lower boundaries of inversion layer	monostatic sodar Aerovironment Model 300	carrier frequency 1600 Hz, sounding height 750 m, vertical resolving ability 17 m	HMICz	the height of inversion layer boundaries is determined from a facsimile record of acoustic echo-signal intensity in the coordinates height-time
mean wind and temperature profiles $u(z)$ and $T(z)$	6 cup anemometers and 6 resistance thermometers with aspiation	cup anemometers M-25 modified by IPA, platinum thermometers TSP 8048	IPA, U.S.S.R.	sensors were placed on the mast at heights from 1 to 32 m. Profiles data processing was carried out by an automatized system including the microcalculator B-3-21

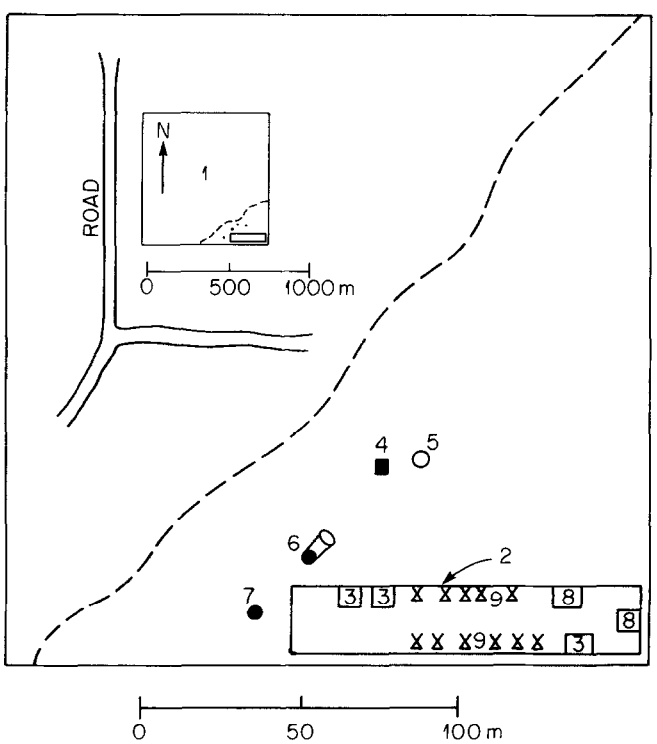

Fig. 1. Lay-out of the ITCE-81 site. (1) experimental area; (2) area where laboratory facilities (3), habitable premises (8), and tents (9) are placed; (4, 5) masts for profile and fluctuation measurements; (6) IPA sodar; (7) $HMIC_z$ sodar.

During the experiment, the weather was mostly warm, anticyclonic and cloudless. Only between July 11 and July 14, 1981, was the weather somewhat different: gusty north and northeast winds, and at times cloudy and rainy (mainly at night). During this period, the temperature fell from 30 to 18 °C. Subsequently, the temperature began to rise (up to 38 °C on July 22) and the weather became mostly cloudless again. The surface wind was usually from 4 to 7 m sec^{-1}.

4. Comparison of Instruments Measuring Wind Velocity and Temperature Fluctuations

Sensors were placed close to each other on masts 4 and 5 (see Figure 1) at a fixed height (4 m or 2 m); then the results of simultaneous measurements of atmospheric turbulence characteristics by different instruments were compared with each other.

Signals from the instruments were received by an IPA digital processing system and recorded on an IPA tape recorder. Those signals from MMO sensors were also received by a MMO analogue processing system and recorded on a MMO tape recorder. All measurements were taken in 34-min runs.

When processing experimental data by the IPA multi-channel digital system, variances and fluxes were determined within each run for two different values of the lower end point of the selected frequency band. The first of these values corresponds to a full 34-min duration of the run and corresponds to 4.9×10^{-4} Hz. The second corresponds to the 256 sec duration of the time intervals into which each run was divided. Variances and fluxes were evaluated for every such interval and then the results were averaged over all the intervals within a run. In this case, the lower end point of a frequency band was equal to 3.9×10^{-3} Hz. Filters with frequency bands extending up from the frequency 3.3×10^{-3} Hz were used in the MMO analogue system.

Use of two different frequency ranges permitted us to discover a considerable drift (as compared to the drifts of MMO instruments) of the mean levels of u and w signals from the IPA acoustic anemometer. Subsequent investigation of this effect showed that this drift was related to defects of a set of acoustic microphones in the IPA anemometer used in the course of the present experiment.

The drift depends on the mean temperature variability and is small enough not to affect noticeably the measured values of the variances σ_u^2 and σ_w^2. However, since the drift is the same both for u and w, there were sometimes considerable distortions of the value of $u_* = \overline{-u'w'}^{1/2}$. Therefore the results of u_* measurements by the IPA sensor were not used.

Figure 2 presents examples of comparisons of σ_u^2, σ_T^2, and $\overline{w'T'}$ values measured by the IPA and MMO instruments. The agreement is quantitatively described by the coefficients a_i and b_i of the regressions $y = a_i x + b_i$ and by the correlation coefficients r_i between x and y, where x and y are the values of the same variable i obtained from the measurements by different instruments. Values of the coefficients a, b, and of r are given in Table II.

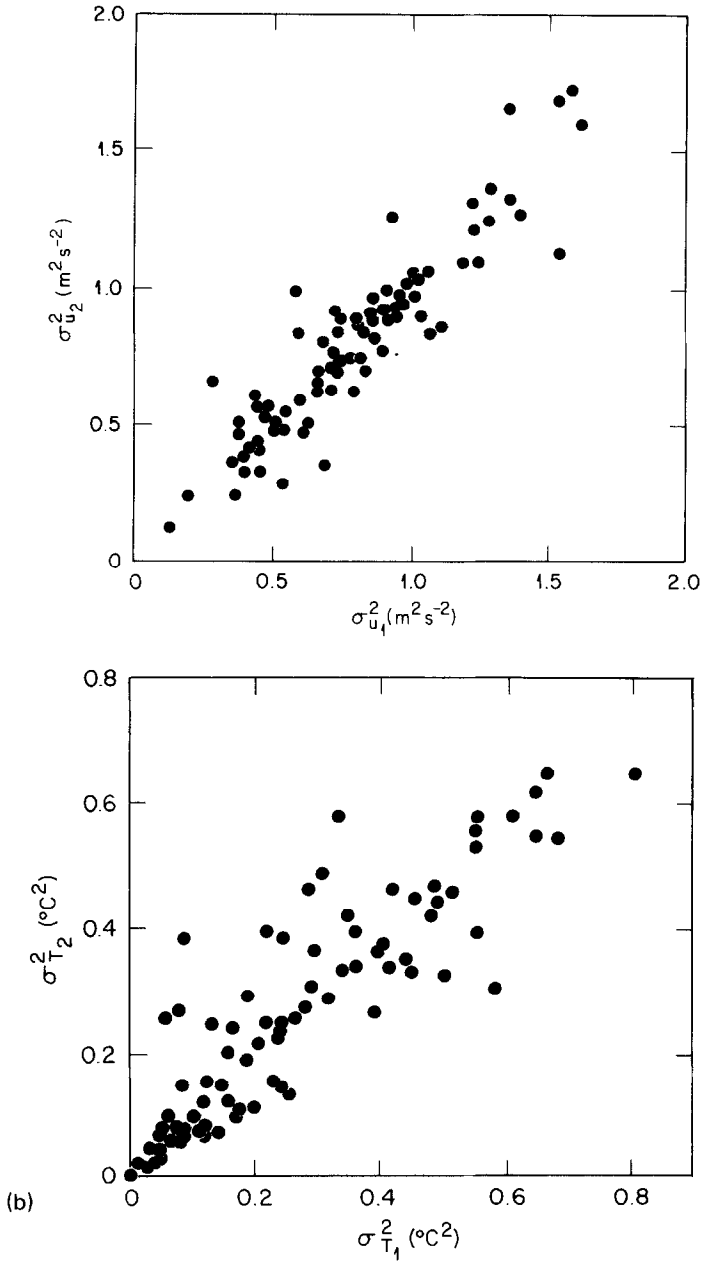

In Figure 3 typical examples of the autospectra F_w, F_u, and F_T (normalized by the corresponding variables) are given for the fluctuation measurements obtained from the IPA, MMO and WPI instruments. Comparison of the results presented in Figure 3 with those in Table II indicates that the discrepancies demonstrated in Table II cannot be

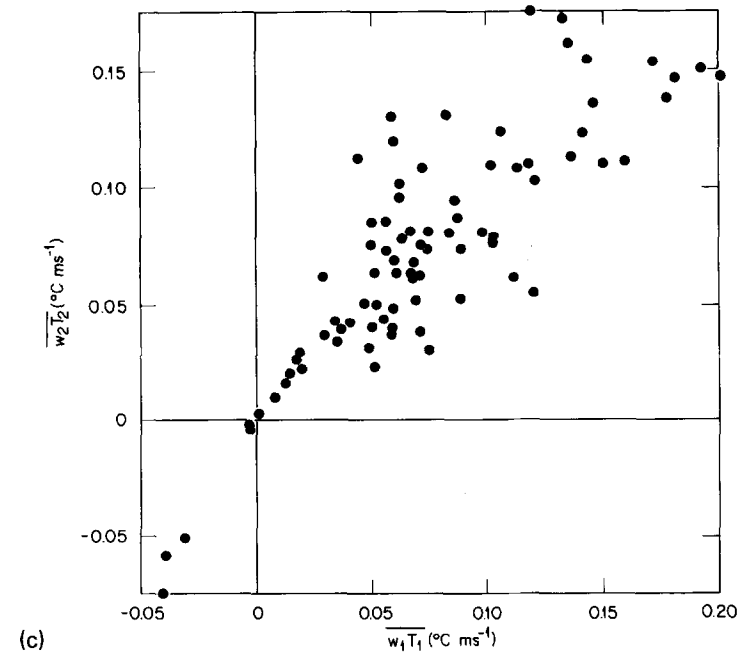

Fig. 2. Comparison of measurements of fluctuation variances σ_u^2, σ_T^2 and turbulent fluxes $\overline{w'T'}$: (1) IPA data; (2) MMO data.

explained in terms of instrumental distortions of the spectral shapes because data from the different instruments lead to shapes that are close to each other over the whole range of measured frequencies. The only exception in this respect is the discrepancies in spectral densities F_{w1} and F_{w2} at frequencies $f \leq 3 \times 10^{-3}$ Hz seen in Figure 3, but we should note that this frequency range contributes not more than 3% to the overall fluctuation variance $\sigma_w = \int_0^\infty F_w \, df$. Therefore the noted discrepancies are negligible when the difference between σ_{w1}^2 and σ_{w2}^2 is estimated.

TABLE II

Regression coefficients a and b and correlation coefficients r between the turbulence characteristics measured by the IPA instruments (index 1), MMO instruments (index 2), and WPI instruments (index 4)

x	y	a	b	r	n
σ_{w1}^2	σ_{w2}^2	1.02	0.01 m^2 s^{-2}	0.89	85
σ_{u1}^2	σ_{u2}^2	0.91	0.07 m^2 s^{-2}	0.95	84
σ_{u1}^2	σ_{u4}^2	0.5	0.36 m^2 s^{-2}	0.75	15
σ_{T1}^2	σ_{T2}^2	0.88	0.03 °C^2	0.93	83
$\overline{w_1' T_2'}$	$\overline{w_2' T_2'}$	0.83	0.01 °C m s^{-1}	0.85	85

Note that all the measurement data (with the above-mentioned exception of the u_* values obtained by IPA instruments) are used in calculations of the coefficients given in Table II.

It is interesting to compare the results obtained in ITCE-81 with the results obtained in ITCE-76 (Australia) (Dyer *et al.*, 1982), particularly the regressions for σ_u^2, σ_w^2, σ_T^2, and $\overline{w'T'}$ values obtained from different instruments. From these data the values of the coefficients a, $|b|$, and r were calculated for each pair of instruments and then their arithmetic means for all the instrument pairs were determined. The results of these calculations are given in Table III.

TABLE III

Mean values of regression coefficients $\bar{a}$, $|\bar{b}|$ and correlation coefficients $\bar{r}$ for ITCE-76 data (Dyer *et al.*, 1976)

Compared characteristics	$\bar{a}$	$\lvert\bar{b}\rvert$	$\bar{r}$	Number of averaged regression graphs
σ_w^2	0.79 ± 0.08	0.04 ± 0.06 m s^{-2}	0.83 ± 0.13	5
σ_u^2	0.83 ± 0.08	0.10 ± 0.05 m^2 s^{-2}	0.93 ± 0.03	5
σ_T^2	0.88 ± 0.13	0.02 ± 0.02 °C^2	0.97 ± 0.01	5
$\overline{w'T'}$	0.88 ± 0.20	0.01 ± 0.009 °C m s^{-1}	0.94 ± 0.03	6

Comparison of Tables II and III shows that in both experiments (ITCE-81 and ITCE-76) the results of measurements of turbulence characteristics with different instruments agree (between themselves) with approximately the same degree of accuracy (characterized by the deviations of the coefficients a and r from unity and of b from zero). Only the measurements of σ_4^2 by the MPI thermoanemometer and by acoustic anemometers (IPA and MMO) are in somewhat worse agreement, though the spectral shapes obtained by these two types of instruments agree satisfactorily with each other (see Figure 3).

Not only the instruments for wind velocity and temperature fluctuation measurements, but also the digital (IPA) and analogue (MMO) systems for data processing were compared in ITCE-81. The signals received from the MMO sensors were treated simultaneously by both systems. The following values of a, b, and r coefficients resulted from the regression analysis applied to u_* measurements: $a = 0.99$; $b = 0.04$ m s^{-1}; $r = 0.90$.

Thus, one can state that both systems used for data processing give results which agree satisfactorily with each other.

5. Comparison of Sodar and in situ Methods of Wind Velocity Measurements

The first successful experiments on scattering of sound by atmospheric turbulence (Kallistratova, 1961) demonstrated that this scattering can be fruitfully used in boundary-

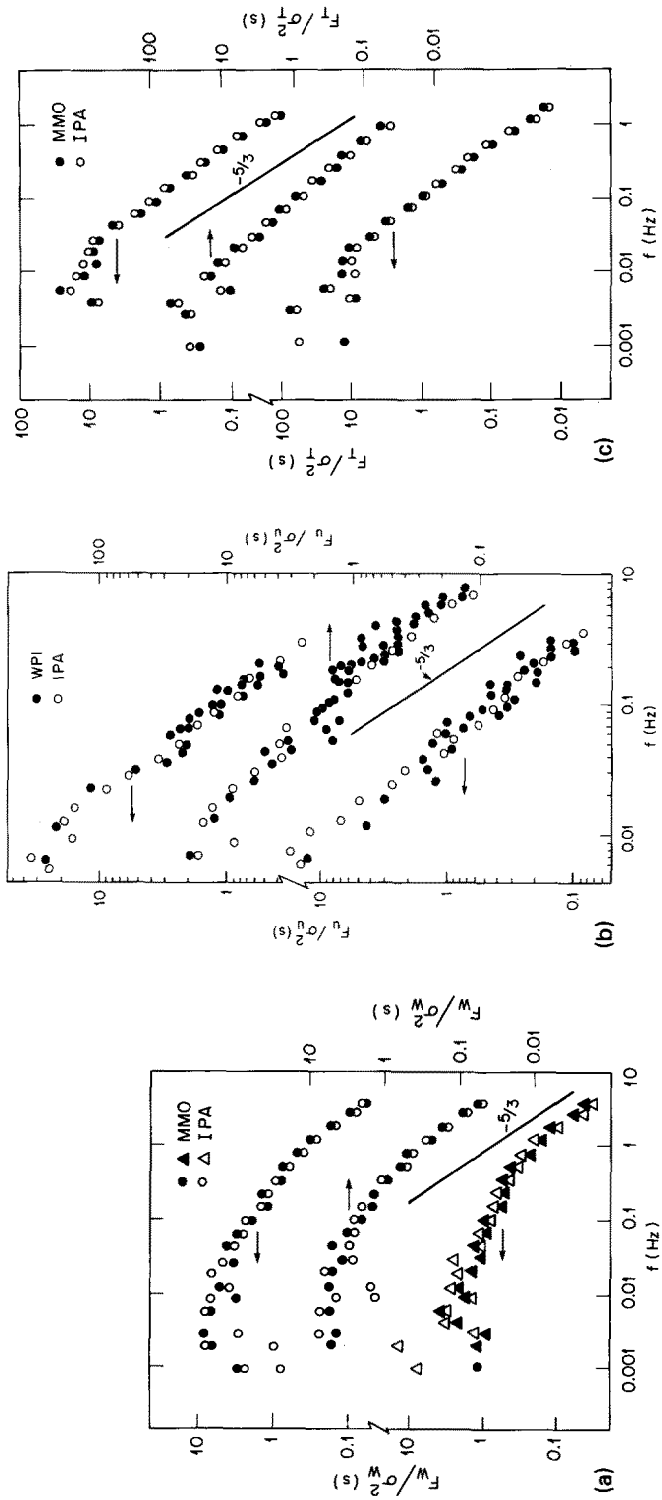

Fig. 3. Examples of normalized spectra of the two wind components and temperature evaluated from the data by IPA, MMO, and WPI. (a) spectra of the vertical wind component obtained by IPA electronic computer; (b) spectra of the longitudinal wind component obtained by IPA and WPI electronic computers; (c) temperature spectra obtained by IPA electronic computer.

layer research. The development of acoustic sounding methods in Australia and USA has resulted in sodars which at present are widely used in the study of atmospheric physics. To obtain quantitative data on the vertical structure of turbulence and wind, it is necessary to determine the real accuracy of sodar measurements by comparison with in-situ measurements.

For ITCE-81, the vertical profiles of longitudinal U_x and lateral U_y wind velocity components (in relation to the wind direction at 4 m height) were determined successively, by rotating the IPA sodar axis by an angle of 90°.

Time-averaged wind velocity components were calculated from the mean Doppler shift Δf of scattered signal frequency f under the assumption that the vertical wind velocity component was negligible:

$$\overline{U}_x(z) = \frac{\Delta f(z)}{f} \frac{C_s}{\cos\theta}$$

where z is the altitude, C_s is sound velocity, and θ is the slope of the sodar axis with respect to the horizon. Then two successive measurements were used to obtain the quantities

$$|\overline{\mathbf{U}(z)}| = (\overline{U_x(z)}^2 + \overline{U_y(z)}^2)^{1/2}; \quad \overline{\varphi(z)} = \operatorname{arctg}(\overline{U_y(z)}/\overline{U_x(z)}).$$

Averaging was over 8.7 min intervals, i.e., over 150 sound pulses generated every 3.5 s*. The minimum interval between runs was 10 min.

Figure 4 shows a comparison between the values $|\overline{\mathbf{U}}|$ at 36 m height (averaged over the layer 30–42 m) and the values $\overline{U}_m$ measured by a cup anemometer placed on a mast at 32 m height. The readings from the cup anemometer were averaged over 17 min. The dotted regression line in Figure 4 is described by the equation

$$|\overline{\mathbf{U}}| = -0.55\ \mathrm{ms}^{-1} + 1.2\,\overline{U}_m .$$

The correlation coefficient between the sodar and in-situ measurements is 0.82. This correlation coefficient is somewhat lower than that obtained by Kaimal *et al.* (1980) in a similar comparison, which can be explained by the difference between the space averaging of sodar data and time averaging of in-situ measurements; this difference can be very noticeable at small heights.

The mast profiles (in the range from 2 to 32 m) and the sodar profiles (in the range from 36 to 150–360 m), which usually couple well with each other, were compared with facsimile records of acoustic echo-signal intensity obtained with the HMICz sodar.

In Figure 5 an example of such a comparison is shown for morning conditions when the surface inversion rises and convection begins to develop. It is seen in Figure 5 that wind velocity profiles reach their maximum at height H corresponding to the upper boundary of the turbulent mixing layer which produces a maximal intensity of echo-signal. It should be noted that low-level atmospheric jets were regularly observed at night and in the morning hours in cases when the surface layer of intense turbulence was

* Maximum averaging time was determined by the memory of the microcomputer.

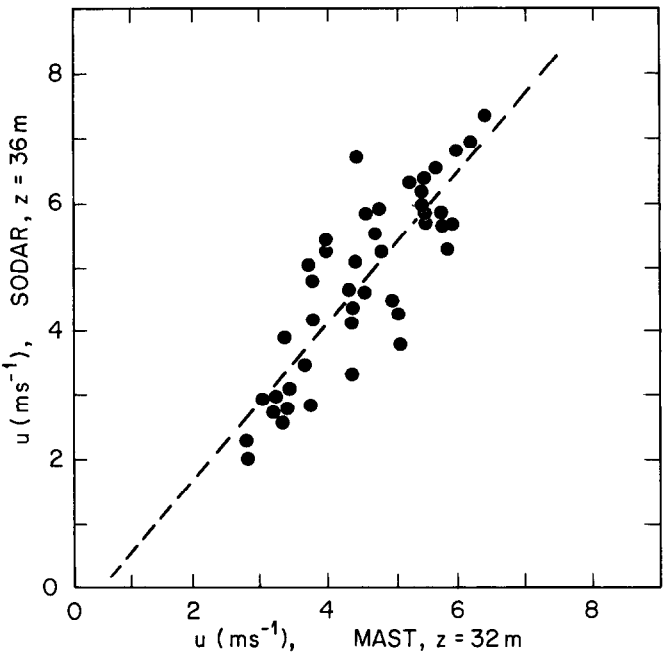

Fig. 4. Comparison of sodar and in-situ (mast) measurements of mean wind velocity. The dotted line represents a linear regression equation $\overline{U}$ (sodar) = $-0.55\ \mathrm{ms}^{-1} + 1{,}2\ \overline{U}$ (mast); correlation coefficient $r = 0.82$.

clearly seen on the facsimile record. The height of the maximum wind velocity was always close to H in such cases. Also, the rate of change of the wind direction with height changed sign at the same height H.

A detailed description of the IPA doppler sodar has been presented by Azizyan *et al.* (1984). Results of sodar measurements were compared with in-situ measurement and with facsimile records in a paper by Kallistratova *et al.* (1984).

6. Similarity Relationships for Wind and Temperature Profiles in Unstable Stratification

One of the purposes of the ITCE-81 was to perform a new determination of the universal functions of the Monin–Obukhov similarity theory related to wind velocity and temperature profiles and to check various correlations proposed in the available literature for the dependence of the momentum and heat fluxes on the vertical gradients of the mean meteorological fields. The measurements were taken mostly in day-time, so the case of unstable stratification will be considered. Many of the similarity relationships proposed for this stratification strongly disagree with each other (see, e.g., a survey paper by Yaglom, 1977); in particular, only some of the suggested forms of the universal functions agree with the asymptotic laws which follow from the free convection theory in a case of strongly unstable stratification.

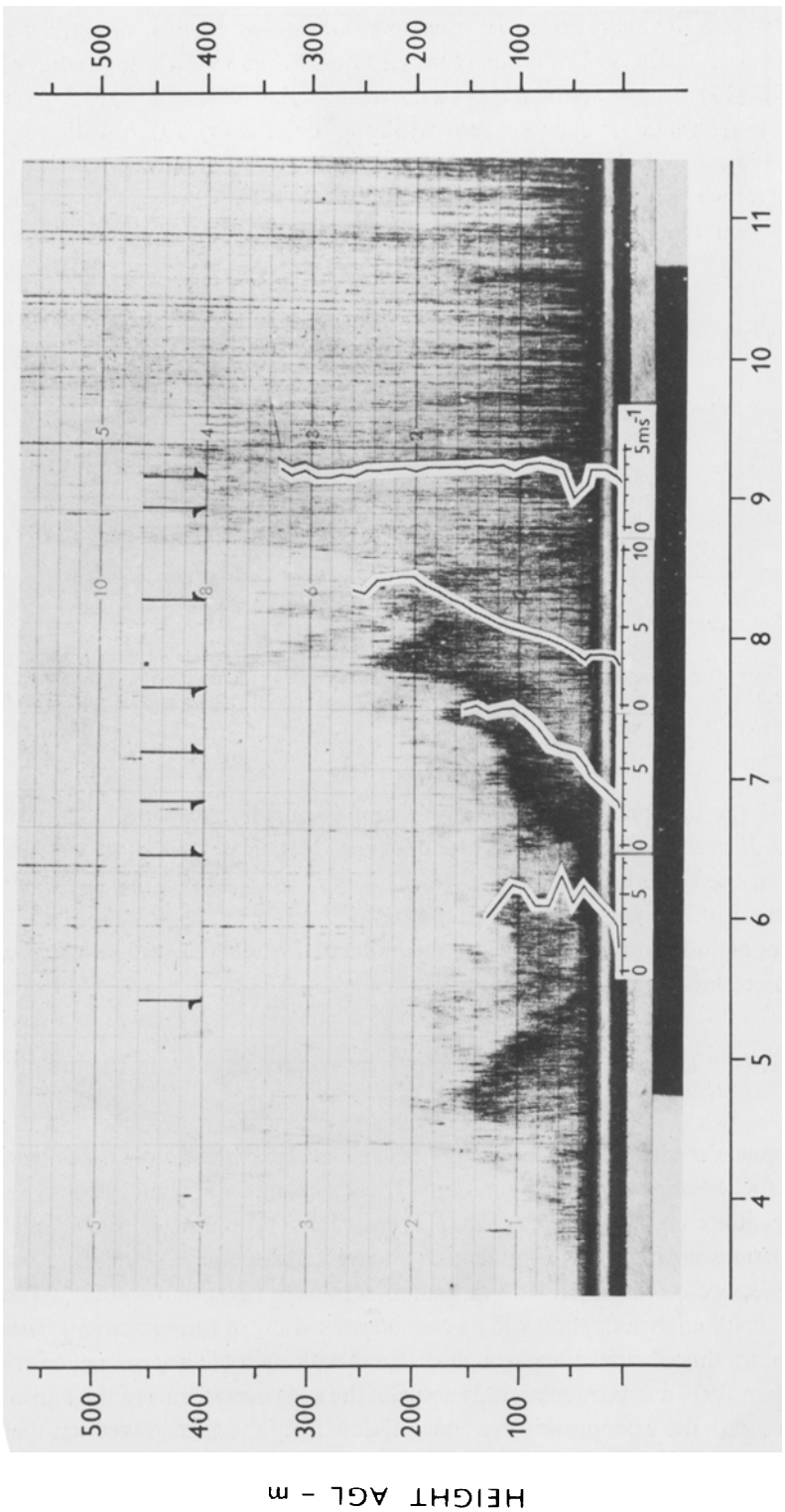

Fig. 5. Example of low-level jet formation and decay during the early morning growth and subsequent decay of a radiation inversion on July 15, 1981. Measurement time intervals for wind profiles is indicated by pairs of arrows.

Wind velocity $u(z)$ and temperature $T(z)$ were measured at six heights, simultaneously with measurements of the vertical momentum and heat fluxes by the eddy correlation method (see Table I). The values of $u(z)$ were measured at heights z = 1, 2, 4, 8, 16, and 32 m, and the six temperature sensors were displaced upwards by 0.15 m with respect to the wind velocity sensors. The results were averaged over 34 min time intervals and the observed averaged profiles of wind velocity $u(z)$ and potential temperature $\theta(z)$ were approximated by functions of the form

$$\left.\begin{matrix} u(z) \\ \Delta\theta(z) \end{matrix}\right\} = K_1 + \frac{K_2 \ln z + K_3 + K_4 z^{2/3}}{5 + z} , \tag{1}$$

where the coefficients K_1, K_2, K_3, and K_4 for both $u(z)$ and $\Delta\theta(z) = \theta(z) - \theta(2.15\text{ m})$ were determined by the method of least squares. The resulting profile equations were used to calculate the vertical gradients $\mathrm{d}u/\mathrm{d}z$ and $\mathrm{d}\theta/\mathrm{d}z$ and also the Richardson number

$$\mathrm{Ri}(z) = \beta \frac{\mathrm{d}\theta/\mathrm{d}z}{(\mathrm{d}u/\mathrm{d}z)^2} , \tag{2}$$

where $\beta = g/T_0$ is the buoyancy parameter (g = 9.81 m s^{-2} is the gravity acceleration and T_0 is the mean absolute temperature for z = 2.15 m). The gradients and the experimental values of turbulent fluxes $-\overline{u'w'} = u_*^2$ and $\overline{w'T'} = Q$ were also used for the determination of the universal functions

$$\phi_u = \frac{kz}{u_*}\frac{\mathrm{d}u}{\mathrm{d}z} \quad \text{and} \quad \phi_\theta = -\frac{kzu_*}{Q}\frac{\mathrm{d}\theta}{\mathrm{d}z} , \tag{3}$$

of the Obukhov length scale $L = -u_*^3/(k\beta Q)$ and of the dimensionless height $\zeta = z/L$. It was supposed in the course of these determinations that the fluxes u_* and Q was constant within the whole layer of u and T measurements and that the von Karman constant k was equal to 0.4.

Parallel with the measurements of the turbulent fluxes by the eddy correlation method, the values of the friction velocity u_* and temperature flux Q were also determined from the profile data. The values of Ri calculated by Equation (2) at the height of the fluctuation measurements and the empirical forms of the functions $\phi_\theta(\mathrm{Ri})$ suggested by some authors (see Table V below) were used for calculations of the values of u_* and Q from Equations (3). In cases where the forms of the functions $\phi_u(\mathrm{Ri})$ and $\phi_\theta(\mathrm{Ri})$ were not given in the literature, but where forms of $\phi_u(\zeta)$ and $\phi_\theta(\zeta)$ were given, the value ζ was first determined from the value $\mathrm{Ri} = \zeta\phi_\theta(\zeta)/\phi_u^2(\zeta)$ and only then were Equations (3) applied to the evaluation of u_* and Q.

The accuracy of the results obtained in such a way naturally depends not only on the accuracy of measurements, but also on the accuracy of the profile approximations by Equation (1). It was shown by Kader and Perepelkin (1983) that in the cases of strong, moderate and weak thermal instability, the deviations of the approximate wind and temperature profiles of the form (1) from the measured profiles $u(z)$ and $\Delta\theta(z)$ are usually

very small even in cases when $\Delta\theta(z)$ is a non-monotonic function of the height. In most cases, the deviations of the experimental points from the approximating curves did not exceed the experimental accuracy of the profile measurements. The trial calculations showed that the use of the other form of the approximating equation with the same number of undetermined coefficients did not result in noticeable changes of the values of Ri up to heights $z \leq 8$ m. However, the distinctions became appreciable at heights of 16 m and especially 32 m, where often the derivative $d\theta/dz$ even changed its sign. For this reason, the experimental results for $z = 32$ m were excluded from the treatment below.

The method of selection of experimental runs for further statistical analysis is also of great importance. In this paper, the results of all the fluctuation measurements with the Kaijo Denki anemometer were taken into account with the exception only of runs characterized by a trend of $\overline{w'T'}$ or $\overline{u'w'}$ exceeding 20%. Also, all results of profile measurements by IPA instruments were used except those for which the velocity and temperature sensors were found to be situated in the wind wake of the mast. After these exclusions, 57 runs (about 85% of all the experiments) remained; they will be used for further analysis.

Summary graphs were then plotted to demonstrate the dependence of universal functions for velocity and temperature on the dimensionless coordinate $\zeta = z/L$ and on Ri. It appeared that experimental data were rather scattered (the scatter was close to 80% in extreme cases and was about 30% on average). To obtain more definite results,

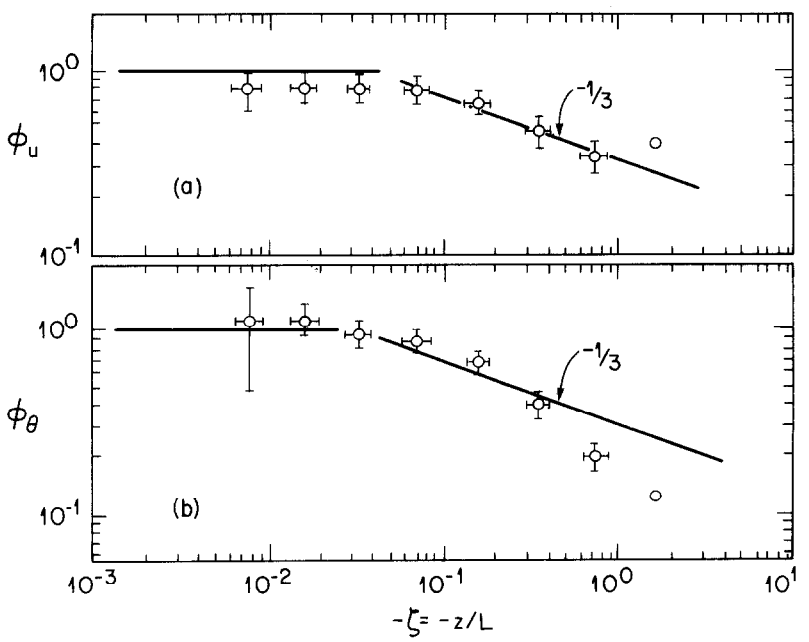

Fig. 6. Universal functions $\phi_u(\zeta)$ and $\phi_\theta(\zeta)$ from the IPA profile measurements and MMO measurements of momentum and heat fluxes. Solid lines indicate asymptotic relations: $\phi_u = 1$, $\phi_\theta = 1$ (for logarithmic sublayer), $\phi_u \sim (-\zeta)^{-1/3}$, $\phi_\theta \sim (-\zeta)^{-1/3}$ (for the case of free convection conditions).

the argument range was partitioned into 11 intervals of the same width on a logarithmic scale. For each of these intervals, the mean values of the function and of the argument were calculated and also the 95% confidence intervals were determined by standard statistical techniques (in cases where there were less than 5 experimental points within the interval, the confidence intervals were not calculated). Figures 6 and 7 show the results.

Comparison of the experimental results plotted in these figures with the theoretical asymptotic laws also represented on the figures shows that the experimental data agree satisfactorily with theoretical predictions on the behavior of the wind velocity and temperature profiles at neutral and strongly unstable stratification. Nevertheless, some other results were found in the course of such a comparison, as mentioned below:

(1) As predicted by Monin–Obukhov theory, the dependence of the dimensionless values of temperature and velocity gradients on the dimensionless height $\zeta = z/L$ can be described by single 'universal functions'.

(2) At $z \leq 0.02|L|$, velocity and temperature profiles are rather accurately described by a logarithmic law. The values of corresponding universal functions $\phi_u(\zeta)$ and $\phi_\theta(\zeta)$ are found to be practically constant in this range of heights and their deviations from unity are statistically insignificant. Hence, the experimental value of the von Karman constant does not differ significantly from the value $k = 0.4$ used in the course of profile treatment by the computer. This last conclusion agrees well with the results of the analogous Australian experiment ITCE-76 described in the papers by Francey and

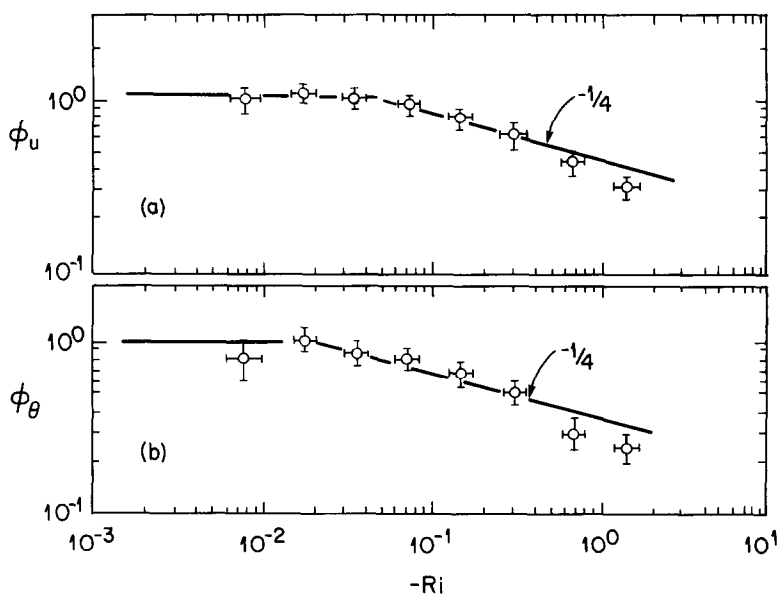

Fig. 7. Universal functions $\phi_u(\mathrm{Ri})$ and $\phi_\theta(\mathrm{Ri})$ from the IPA profile measurements and MMO measurements of momentum and heat fluxes. Solid lines indicate asymptotic relations: $\phi_u = 1$, $\phi_\theta = 1$ (for the logarithmic sublayer, $\phi_u \sim (-\mathrm{Ri})^{-1/4}$, $\phi_\theta \sim (-\mathrm{Ri})^{-1/4}$ (for the case of free convection conditions).

Garratt (1981) and Dyer and Bradley (1982) and with the results of Kondo and Sato (1982) who considered this problem especially.

(3) The fact that the experimental points in Figure 6 in the range $-0.03 \geq \zeta \geq -0.5$ are grouped rather well along a straight line with slope $-1/3$ shows that at the heights $0.03|L| \leq z \leq 0.5|L|$, the free convection laws are valid with satisfactory accuracy (c.f.Monin and Yaglom, 1971, Section 7.3). Note, however, that this agreement with theory is observed only in a limited range of ζ; with a further increase of $|\zeta|$, experimental points (especially for the function ϕ_θ) begin to deviate from the corresponding straight lines (down in the case of the function $\phi_\theta(\zeta)$ and up in the case of the function $\phi_u(\zeta)$).

(4) A similar conclusion can be drawn from the analysis of the experimental curves in Figure 7, concerning the determining functions $\phi_w(\mathrm{Ri})$ and $\phi_u(\mathrm{Ri})$. The only difference is that the asymptotic free convection laws correspond here to straight lines with slope $-1/4$; at high enough values of $|\mathrm{Ri}|$, the experimental points begin to deviate down from these lines for both $\phi_u(\mathrm{Ri})$ and $\phi_\theta(\mathrm{Ri})$.

The above-mentioned results for wind velocity and temperature profiles can be analysed quantitatively by the following method. Using the available experimental data, we study the influence of ζ- and Ri-ranges on the values of parameters p and q in the approximate equations of the form

$$\left.\begin{matrix}\phi_u \\ \phi_\theta\end{matrix}\right\} = q(-\zeta)^p \quad \text{or} \quad \left.\begin{matrix}\phi_u \\ \phi_\theta\end{matrix}\right\} = q(-\mathrm{Ri})^p \tag{4}$$

and on the accuracy of approximation (4). The results of the corresponding statistical analysis are summarized in Table IV, which shows: (1) values of p and q with 95% confidence range; (2) the number of experimental points n falling into the corresponding ζ- or Ri-range; and (3) the value of the correlation coefficient r between the true values of ϕ_u or ϕ_θ and their approximations (4). (The closeness of r to unity characterizes, of course, the accuracy of the approximating relations (4).)

The values of r collected in Table IV show that the scatter of experimental data for the dimensionless velocity profile $\phi_u(\zeta)$ exceeds considerably the analogous scatter for the temperature profile $\phi_\theta(\zeta)$. This is connected first of all with a different role of the friction velocity u_* entering into the definitions of both the functions ϕ_u and ϕ_θ and the relation $\zeta = z/L$. Therefore, the dependence on u_* can produce erroneous apparent relationships between the functions and their argument (c.f. Hicks, 1981). It follows from theoretical considerations (see, e.g., Monin and Yaglom, 1971, Section 7.3) that at high enough values of $|\zeta|$, the functions ϕ_u and ϕ_θ are proportional to $(-\zeta)^{-1/3}$. Recalling now the definition (3) of these functions, we come to the conclusion that in the region of validity of the free convection laws, the following equations must hold:

$$\frac{kz}{u_*}\frac{\mathrm{d}u}{\mathrm{d}z} \sim \frac{u_*}{(-kz\beta Q)^{1/3}}; \qquad \frac{kzu_*}{Q}\frac{\mathrm{d}\theta}{\mathrm{d}z} \sim \frac{u_*}{(-kz\beta Q)^{1/3}}.$$

Therefore the errors in measured values of u_* (which are apparently the most important ones) distort the form of the function $\phi_u(\zeta)$ but do not affect the form of $\phi_\theta(\zeta)$. An

TABLE IV

Approximation of the velocity and temperature universal functions φ_u and φ_θ by power functions of the form $\varphi_u, \varphi_\theta = q(-\zeta)^p$ or $\varphi_u, \varphi_\theta = q(-\mathrm{Ri})^p$

Function	Range of the argument	n	r	$p + \Delta p_{0.95}$	$q + \Delta q_{0.95}$
$\varphi_u(\zeta)$	$\zeta < -0.03$	238	0.63	-0.32 ± 0.06	0.34 ± 0.02
	$-0.5 < \zeta < -0.03$	176	0.43	-0.17 ± 0.06	0.52 ± 0.02
$\varphi_\theta(\zeta)$	$\zeta < -0.03$	238	0.84	-0.52 ± 0.04	0.19 ± 0.01
	$-0.5 < \zeta < -0.03$	176	0.75	-0.33 ± 0.04	0.31 ± 0.01
$\varphi_u(\mathrm{Ri})$	$\mathrm{Ri} < -0.03$	238	0.85	-0.31 ± 0.02	0.37 ± 0.01
	$-0.5 < \mathrm{Ri} < -0.03$	171	0.62	-0.22 ± 0.04	0.47 ± 0.02
$\varphi_\theta(\mathrm{Ri})$	$\mathrm{Ri} < -0.03$	238	0.76	-0.38 ± 0.04	0.27 ± 0.02
	$-0.5 < \mathrm{Ri} < -0.03$	171	0.55	-0.23 ± 0.05	0.41 ± 0.02

analogous analysis of the influence of the temperature flux Q shows that possible errors in its determination affect the form of ϕ_θ in a free convection region more strongly than ϕ_u; however, these errors are usually not very consequential and play only a minor role. To exclude the influence of the errors in measured values of u_* and Q on the forms of dimensionless empirical velocity and temperature profiles deduced from experimental data, the profile data were used to determine the functions $\phi_u(\mathrm{Ri})$ and $\phi_\theta(\mathrm{Ri})$ of Ri (and not of ζ). Note that asymptotic relations $\phi_u \sim (-\mathrm{Ri})^{-1/4}$, $\phi_\theta \sim (-\mathrm{Ri})^{-1/4}$ valid at high values of $|\mathrm{Ri}|$ (see, e.g., Monin and Yaglom, 1971) imply the following formulas:

$$\frac{kz}{u_*}\frac{\mathrm{d}u}{\mathrm{d}z} \sim \left(\frac{\mathrm{d}u}{\mathrm{d}z}\right)^{1/2}\left(-\beta\frac{\mathrm{d}\theta}{\mathrm{d}z}\right)^{-1/4};$$

$$\frac{kzu_*}{Q}\frac{\mathrm{d}\theta}{\mathrm{d}z} \sim \left(\frac{\mathrm{d}u}{\mathrm{d}z}\right)^{1/2}\left(-\beta\frac{\mathrm{d}\theta}{\mathrm{d}z}\right)^{-1/4}.$$

It is easy to deduce from these formulas that the appearance of the measured values of gradients $\mathrm{d}u/\mathrm{d}z$ and $\mathrm{d}\theta/\mathrm{d}z$ both in the definitions of the functions ϕ_u, ϕ_θ and in their arguments must lead to a greater scatter of experimental points in the graph for $\phi_\theta(\mathrm{Ri})$ than in the graph for $\phi_u(\mathrm{Ri})$. Inspection of the corresponding values of the correlation coefficient r presented in Table IV confirms this conclusion.

The calculated values of the exponent p corresponding to the entire body of analysed data appear to be close enough to the values of the same exponent obtained in a number of other papers (see, e.g., the equations for ϕ_u and ϕ_θ given in the papers by Businger *et al.*, 1971; Dyer and Hicks, 1970; and Dyer and Bradley, 1982). Thus according to Dyer and Bradley $p = -0.214 \pm 0.016$ for $\phi_u(\zeta)$ and $p = -0.518 \pm 0.059$ for $\phi_\theta(\zeta)$, while for the present data, p is also close to -0.3 for $\phi_u(\zeta)$ and close to -0.5 for $\phi_\theta(\zeta)$. Note also that experimental values of p differ from the values predicted by free convection theory: $p = -1/3$ for $\phi_u(\zeta)$ and $\phi_\theta(\zeta)$, and $p = -1/4$ for $\phi_u(\mathrm{Ri})$ and $\phi_\theta(\mathrm{Ri})$.

However, the values of exponents p in the power approximations to $\phi_u(\zeta)$, $\phi_\theta(\zeta)$, $\phi_u(\mathrm{Ri})$, and $\phi_\theta(\mathrm{Ri})$ calculated only for the range $-0.03 \geq \zeta \geq -0.5$ are in good agreement with theoretical predictions related to free convection. (The only exception is the value of p in the power approximation of $\phi_u(\zeta)$, but the low values of r and the large confidence intervals indicating considerable data scatter make the corresponding value of p rather suspicious.)

Thus according to the experimental data, the sublayer of the unstably stratified atmospheric surface layer, in which free convection laws are valid is bound from below and from above. This conclusion contradicts theoretical predictions by Prandtl (1932), Obukhov (1946, 1960) and Priestley (1959) who obtained the free convection laws as asymptotic laws for $z \to \infty$ based on simple dimensional considerations. Later Zilitinkevich (1971) and Betchov and Yaglom (1971) tried to apply to the study of the unstably stratified surface layer, the concept of a length dimension depending on the considered direction (differing for the horizontal and the vertical coordinate axis). They came to the conclusion (based on some plausible assumptions) that the zone where free convection laws are valid has apparently a two-layer structure. In the lower free convection sublayer (which apparently ranges from a height close to $0.03\,|L|$ up to a height of the order $|L|$), horizontal velocity fluctuations are generated mostly by the wind shear and therefore they are strongly affected by the value of u_*; however, fluctuations w' are determined mainly by thermal convection, so that u_* becomes unessential for these fluctuations. Above this layer (but still within the range where momentum and heat fluxes are practically independent of height), a pure convection sublayer is situated where u_* plays no role at all in turbulence production and the theoretical conclusions by Prandtl, Obukhov, and Priestley are fully applicable. If so, then the relations $\phi_u \sim (\zeta)^{-1/3}$ and $\phi_\theta \sim (-\zeta)^{-1/3}$ must be valid in both the free convection and pure convection sublayers, but there are no reasons to expect that the coefficients of proportionality in these formulas are also equal for the two sublayers. If these coefficients differ considerably, then the approximation for the functions $\phi_u(\zeta)$ or $\phi_\theta(\zeta)$ in the whole range of ζ, which includes both the sublayers and also a transition zone between them, by the unique power law of the form (4) will result in the value of p differing considerably from the theoretical value $p = -1/3$.

Graphs in Figures 6 and 7 and the results given in Table IV agree satisfactorily with this conclusion. Summing up the results of this statistical analysis, it can be concluded that according to experimental data, the free convection sublayer at the bottom of the unstably stratified surface layer apparently ranges from -0.03 to $-0.5\,L$ (or from $\mathrm{Ri} \approx -0.03$ to $\mathrm{Ri} \approx -0.5$). This agrees rather well with crude theoretical estimates by Betchov and Yaglom (1971) and with the results of Webb (1958, 1982) who was apparently the first to indicate that the free convection law $\mathrm{d}\theta/\mathrm{d}z \sim z^{-4/3}$ is valid in the range $-0.03 \geq \mathrm{Ri} \geq -0.4$, but does not hold for further increases of $|\mathrm{Ri}|$ (see also Monin and Yaglom, 1971, Section 8.2).

Let us now compare measured values of momentum and temperature fluxes u_*^2 and Q with their values determined from the mean profile data with the aid of specific forms of the universal functions ϕ_u and ϕ_θ suggested by various authors for the case of unstable

TABLE V

Flux-profile relationships suggested by various authors

Priestley (1959)	$\varphi_\theta = \begin{cases} 1 \\ 0.32(-\zeta)^{-1/3} \end{cases}$	at at	$0 \geq \mathrm{Ri} \geq -0.03$ $\mathrm{Ri} < -0.03$
Zilitinkevich and Chalikov (1968)	$\varphi_u, \varphi_\theta = \begin{cases} 0.93(1+1.56\zeta) \\ 0.38(-\zeta)^{1/3} \end{cases}$	at at	$0 \geq \zeta \geq -0.15$ $-0.15 \geq \zeta \geq -1.2$
Dyer and Hicks (1970)	$\varphi_u = 0.98(1-16.4\zeta)^{-1/4}$ $\varphi_\theta = 0.98(1-16.4\zeta)^{-1/2}$	at at	$0 \geq \zeta \geq -2$ $0 \geq \zeta \geq -2$
Businger *et al.* (1971)	$\varphi_u = 1.14(1-13.1\zeta)^{-1/4}$ $\varphi_\theta = 0.84(1-7.9\zeta)^{-1/2}$	at at	$0 \geq \zeta \geq -2$ $0 \geq \zeta \geq -2$
Pruitt *et al.* (1973)	$\varphi_u = 0.95(1-16\mathrm{Ri})^{-1/3}$ $\varphi_\theta = 0.84(1-22\mathrm{Ri})^{-0.4}$	at at	$0 \geq \mathrm{Ri} \geq -3.5$ $0 \geq \mathrm{Ri} \geq -3.5$
Skeib (1980)	$\varphi_u = \begin{cases} 1 \\ (-\zeta/0.075)^{-1/4} \end{cases}$	at at	$0 \geq \zeta \geq -0.075$ $-0.075 \geq \zeta \geq -2.5$
	$\varphi_\theta = \begin{cases} 0.8 \\ 0.8(-\zeta/0.075)^{-1/2} \end{cases}$	at at	$0 \geq \zeta \geq -0.075$ $-0.075 \geq \zeta \geq -2.5$
Gavrilov and Petrov (1981)	$\varphi_u = (1-8\zeta)^{-1/3}$ $\varphi_\theta = 0.65(1-35\zeta)^{-1/3} + [4(1+8\zeta^2)]^{-1}$	at at	$\zeta \leq 0$ $\zeta \leq 0$

stratification. The relations to be considered are summarized in Table V. A statistical test of these relations was carried out by computing the regression equations:

$$u_{*\mathrm{cal}}^2 = a_2 u_{*m}^2 + b_1 ; \qquad Q_{\mathrm{cal}} = a_2 Q_m + b_2 .$$

(See the examples presented in Figures 8 and 9.)

Table VI contains the values of the coefficients a_1, b_1 and a_2, b_2 determined by the method of least squares together with the corresponding 95% confidence intervals.

It should be noted that the variability of the tested relations increased considerably with an increase of $|\mathrm{Ri}|$. Thus, for example, at $\mathrm{Ri} \sim -1$ some of the calculated fluxes obtained from different relations differ by more than a factor of two, while at low values of $|\mathrm{Ri}|$ all the relations give practically the same results. Therefore the large number of data points related to nearly neutral stratification may lead to the erroneous conclusion that on average, there is good agreement among the predictions and with experimental data. In order to avoid such an undue influence of the numerous measurements at small values of $|\mathrm{Ri}|$, we varied the Ri-range and calculated separately the results for different ranges of Ri.

The heat flux calculations implied by the first equation for ϕ_θ in Table V are traditionally based on the use of the Priestley function

$$H_* = Q/(\beta^{1/2} z^2 \, |\mathrm{d}\theta/\mathrm{d}z^{3/2}) .$$

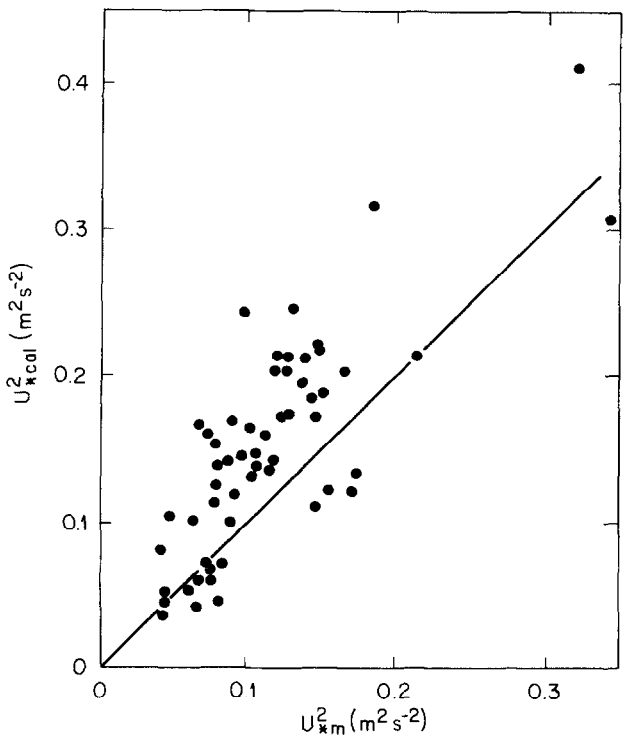

Fig. 8. Comparison of u_*^2 based on the IPA profile measurements and Dyer and Hicks' universal functions (1970).

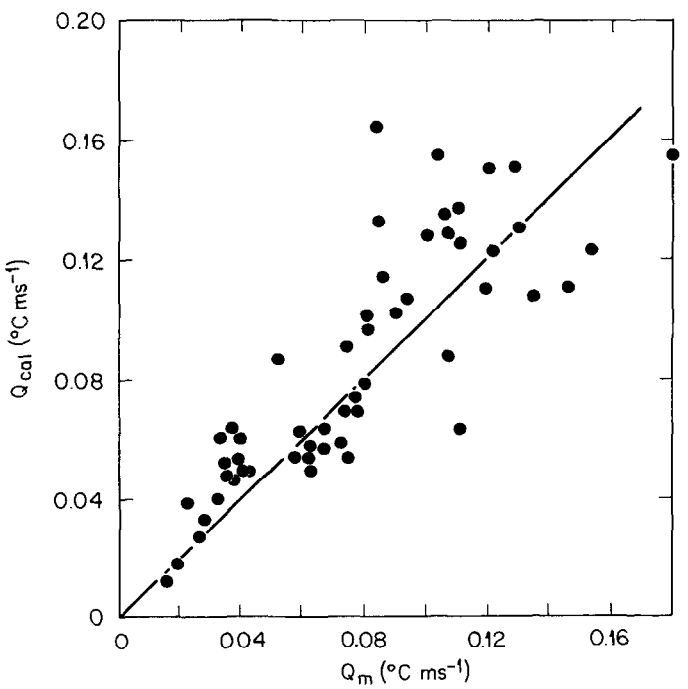

Fig. 9. Comparison of Q based on the IPA profile measurements and Priestley's model equations (1959).

TABLE VI

Comparison of directly measured momentum and temperature fluxes with the calculations from the profile measurements implied by various suggested forms of the universal functions φ_u and φ_θ: $u_{*\text{cal}}^2 = a_1 u_{*m}^2 + b_1$; $Q_{\text{cal}} = a_2 Q_m + b_2$

Author(s)	Ri range	n	u_*^2 m^2 s^{-2}			Q °C m s^{-1}		
			r	$a_1 + \Delta a_1$	$b_1 + \Delta b_1$	r	$a_2 + \Delta a_2$	$b_2 + \Delta b_2$
Priestley	Ri < 0	57	–	–	–	0.86	0.94 ± 0.15	0.01 ± 0.01
(1959)	Ri < −0.04	47				0.85	0.93 ± 0.17	0.01 ± 0.01
Zilitinkevich and	Ri < 0	57	0.83	1.07 ± 0.19	0.02 ± 0.01	0.83	0.75 ± 0.13	0.02 ± 0.01
Chalikov (1968)	Ri < −0.04	47	0.67	0.89 ± 0.29	0.03 ± 0.01	0.82	0.77 ± 0.15	0.02 ± 0.01
Dyer and Hicks	Ri < 0	57	0.81	1.01 ± 0.19	0.03 ± 0.01	0.85	1.10 ± 0.18	0.02 ± 0.01
(1970)	Ri < −0.04	47	0.58	0.97 ± 0.31	0.03 ± 0.01	0.84	1.09 ± 0.20	0.02 ± 0.01
Businger *et al.*	Ri < 0	57	0.81	0.76 ± 0.15	0.02 ± 0.01	0.85	0.99 ± 0.16	0.02 ± 0.01
(1971)	Ri < −0.04	47	0.67	0.74 ± 0.24	0.02 ± 0.01	0.84	0.98 ± 0.18	0.02 ± 0.01
Pruitt *et al.*	Ri < 0	57	0.79	1.07 ± 0.22	0.05 ± 0.01	0.85	1.42 ± 0.23	0.02 ± 0.01
(1973)	Ri < −0.04	47	0.67	1.14 ± 0.37	0.04 ± 0.01	0.84	1.40 ± 0.26	0.03 ± 0.01
Skeib (1980)	Ri < 0	57	0.83	0.87 ± 0.15	0.01 ± 0.01	0.82	0.91 ± 0.17	0.02 ± 0.01
	Ri < −0.04	47	0.67	0.68 ± 0.22	0.03 ± 0.01	0.81	0.91 ± 0.20	0.02 ± 0.01
Gavrilov and Petrov	Ri < 0	57	0.82	0.95 ± 0.18	0.02 ± 0.01	0.85	1.00 ± 0.17	0.02 ± 0.01
(1981)	Ri < −0.04	47	0.67	0.88 ± 0.28	0.03 ± 0.01	0.84	0.99 ± 0.19	0.02 ± 0.01

It is easy to see that $H_* =$ constant in free convection and that $H_* \sim (-\text{Ri})^{-1/2}$ in nearly neutral stratification. A graph of the experimental value of the function $H_*(\text{Ri})$ is given in Figure 10. We see that both theoretical asymptotic relations agree well with the data points determined from the measurements by the IPA and MMO groups, but only if $-\text{Ri} \leq 0.5$. At greater values of $-\text{Ri}$, the function $H_*(\text{Ri})$ increases again with $|\text{Ri}|$; this can be explained by the assumption that at $\text{Ri} \approx -0.5$, a transition zone, which separates free convection and the pure convection layer, begins.

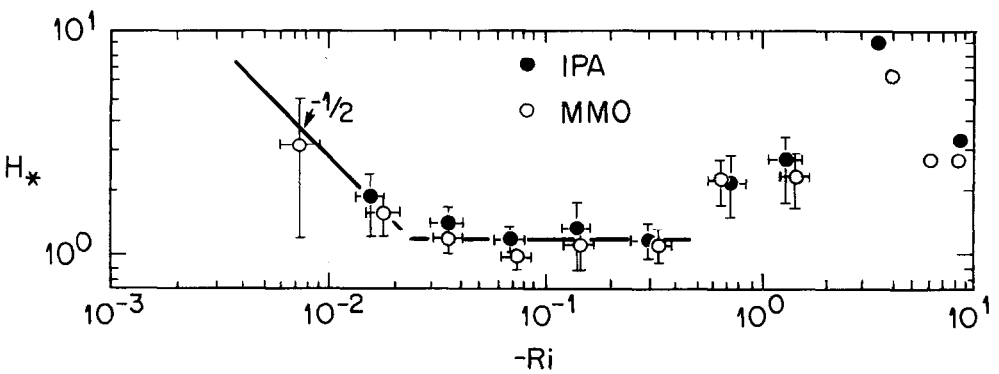

Fig. 10. Dependence of Priestley's function H_* on Ri. Solid lines indicate asymptotic relations $H_* \sim (-\text{Ri})^{-1/2}$ and $H_* =$ const which are valid at forced convection (logarithmic) and free convection conditions.

Statistical analysis of the available experimental data permits us to estimate the coefficients p and H_0 of the relation $H_* = H_0(-\mathrm{Ri})^p$ for various ranges of Ri. Thus, for $0 > \mathrm{Ri} > -0.03$, we obtain $p = -0.52 \pm 0.29$, and $H_0 = 0.18 \pm 0.02$, in good agreement with the theoretical deduction that $p = -0.5$ for small enough $|\mathrm{Ri}|$. Moreover, if $-0.03 > \mathrm{Ri} > -0.05$, then $p = 0.00 \pm 0.06$, $H_0 = 1.01 \pm 0.05$. The value of p clearly agrees well with the prediction of free convection theory that $H_* =$ constant and hence $p = 0$. Note also that the deduced value of H_0 is within the range of the constant values of H_* found earlier (see, e.g., Monin and Yaglom, 1971, Section 8.2).

The data on temperature flux Q obtained in ITCE-81 were also directly compared with Priestley's equation (1959)

$$Q = \begin{cases} 0.16(-\mathrm{Ri})^{-1/2}\beta^{1/2}z^2|\mathrm{d}\theta/\mathrm{d}z|^{3/2} & \text{for} \quad 0 \geq \mathrm{Ri} \geq -0.03 \\ 0.9\beta^{1/2}z^2|\mathrm{d}\theta/\mathrm{d}z|^{3/2} & \text{for} \quad -0.03 > \mathrm{Ri}\,. \end{cases}$$

The results presented in Table VI show that the scatter of the experimental points is too large to permit a recommendation concerning which of the suggested relations is the best. Note also that for the momentum flux u_*^2, the values of the correlation coefficient r decrease considerably when the lower bound of the considered values of $-\mathrm{Ri}$ increases (i.e., when passing from nearly neutral conditions to moderate and strong instability). The equations by Zilitinkevich and Chalikov (1968), Dyer and Hicks (1970), Pruitt *et al.* (1973) and Gavrilov and Petrov (1981) are recommended as giving the best results when applied to the calculation of u_* from profile data.

In the case of heat flux calculations, the value of r does not decrease when the lower bound of the considered range of $-\mathrm{Ri}$ increases. In this case, the various forms for ϕ_θ (except those by Zilitinkevich and Chalikov, 1968, and Pruitt *et al.*, 1973) apparently have nearly the same accuracy (which is, of course, strongly restricted by the scatter of experimental data). The more satisfactory accuracy of heat flux calculations as compared with calculations of the momentum flux can be explained by the fact that errors in the measured values of u_* do not greatly affect the functions $\phi_\theta(\zeta)$ and $\phi_\theta(\mathrm{Ri})$ while errors in the measured values of Q only slightly affect these functions. Therefore, the scatter of experimental data on ϕ_θ is relatively small and various formulas suggested to approximate these data differ only slightly from each other (c.f., e.g., the graphs of the functions $\phi_\theta(\zeta)$, $\zeta \leq 0$, Figure 2 of the review by Yaglom (1977), with much more scattered plots of $\phi_u(\zeta)$, $\zeta \leq 0$, in Figure 1 of the same paper).

7. Conclusions

(1) The ITCE-81 results of measurements of the atmospheric turbulence characteristics by different instruments agree quite satisfactorily with the similar results obtained in the course of the Australian experiment ITCE-76. Both experiments show that even when the measurements are carried out over a rather homogeneous and flat surface in stationary conditions, the measured values of the same quantity obtained by different instruments do not agree very well with each other and their scatter is usually

characterized by correlation coefficients in the range 0.85 to 0.95. This scatter limits the achievable accuracy of measurements of wind velocity and temperature variances and of the turbulent heat and momentum fluxes over a homogeneous underlying surface in stationary, unstable conditions.

(2) It is shown that an unstable stratified atmospheric surface layer has a complicated structure. For heights below $-0.02\,L$, wind velocity and temperature profiles are rather well described by the logarithmic law. For $-0.03 \geq z/L \geq -0.5$, the profiles agree with the free convection law $\phi_u \sim \phi_\theta \sim (-\zeta)^{-1/3}$. At heights $z > -0.5\,L$, the universal functions $\phi_u(\zeta)$ and $\phi_\theta(\zeta)$ begin to deviate from this theoretical law.

(3) Statistical comparison of measured values of the turbulent fluxes u_*^2 and Q with values calculated from the model equations for ϕ_u and ϕ_θ suggested by different authors allows recommendations to be made concerning which are the most accurate models.

Acknowledgements

The authors are thankful to Prof. A. M. Yaglom for many useful discussions and for help in the preparation of the English text of the paper.

References

Azizyan, G. V., Kallistratova, M. A., Martvel', F. E., Petenko, I. V., and Time, N. S.: 1983, 'Sodar Anemometer', *Izv. Akad. Nauk SSSR, Fiz. Atm. i Okeana* (Bull. Acad. Sci. USSR, Atmospheric and Oceanic Physics) **20**, 100–104.

Betchov, R. and Yaglom, A. M.: 1971, 'Comments on Similarity Theory for Turbulence in Unstably Stratified Fluid', *Izv. Akad. Nauk SSSR, Fiz. Atm. i Okeana* (Bull. Acad. Sci. USSR, Atmospheric and Oceanic Physics) **7**, 1270–1279.

Businger, J. A., Miyake, M., Dyer, A. J., and Bradley, E. F.: 1967, 'On the Direct Determination of the Turbulent Heat Flux Near the Ground', *J. Appl. Meteorol.* **6**, 1025–1032.

Businger, J. A., Wyngaard, J. C., Izumi, Y., and Bradley, E. F.: 1971, 'Flux-Profile Relationships in the Atmospheric Surface Layer', *J. Atmos. Sci.* **28**, 181–189.

Dyer, A. J. and Bradley, E. F.: 1982, 'An Alternative Analysis of Flux-Gradient Relationships at the 1976 ITCE', *Boundary-Layer Meteorol.* **22**, 3–19.

Dyer, A. J. and Hicks, B. B.: 1970, 'Flux-Gradient Relationships in the Constant Flux Layer', *Quart. J. Roy. Meteorol. Soc.* **96**, 715–721.

Dyer, A. J., Garratt, J. R., Francey, R. J., McIlroy, I. C., Bacon, N. E., Hyson, P., Bradley, E. F., Denmead, O. T., Tsvang, L. R., Volkov, Y. A., Koprov, B. M., Elagina, L. G., Sahashi, K., Monji, N., Hanafusa, T., Tsukamoto, O., Frenzen, P., Hicks, B. B., Wesely, M., Miyake, M., and Shaw, W.: 1982, 'An International Turbulence Comparison Experiment (ITCE 1976)', *Boundary-Layer Meteorol.* **24**, 181–209.

Francey, R. J. and Garratt, J. R.: 1981, 'Interpretation of Flux-Profile Observation at ITCE (1976)', *J. Appl. Meteorol.* **20**, 603–618.

Gavrilov, A. S. and Petrov, Y. S.: 1981, 'Accuracy of the Estimates for Turbulent Fluxes Measured Over the Sea by Standard Hydrometeorological Instruments', *Meteor. i Gidrol.* (Meteorology and Hydrology) No. 4, 52–59.

Hicks, B. B.: 1981, 'An Examination of Turbulence Statistics in the Surface Boundary Layer', *Boundary-Layer Meteorol.* **21**, 389–402.

Kader, B. A., and Perepelkin, V. G.: 1984, 'Wind Velocity and Temperature Profiles in the Atmospheric Surface Layer at a Neutral and Unstable Stratification', *Izv. Acad. Sci. USSR, Atmosph. and Oceanic Phys.* **20**, 151–161.

Kaimal, J. C., Gaynor, J. E., and Baynton, H. W.: 1980, 'Summary of Results. The Boulder Low-Level Intercomparison Experiment 1979', Report No. 3 of World Met. Org., Geneva, 155–191.

Kallistratova, M. A.: 1961, 'Experimental Investigation of Sound Wave Scattering in the Atmosphere' (in Russian), Tr. Inst. Fiz. Atmos., *Atmos. Turbulentnost* **4**, 203–256. (English Translation by US Air Force FTD TT63-441.)

Kallistratova, M. A., Keder, J., Petenko, I. V., and Time, N. S.: 1985, 'Measurements of Mean Wind Profiles by a Sodar Anemometer', *Izv. Akad. Nauk SSSR, Fiz. Atmos. i Okeana* (Bull. Acad. Sci. USSR, Atmospheric and Oceanic Physics) (in press).

Kondo, J. and Sato, T.: 1982, 'The Determination of the von Kármán Constant', *J. Meteorol. Soc. Japan, Ser. II*, **60**, 461–471.

Miyake, M., Stewart, R. W., Burling, H. W., Tsvang, L. R., Koprov, B. M., and Kuznetsov, O. A.: 1971, 'Comparison of Acoustic Instruments in an Atmospheric Turbulent Flow over Water', *Boundary-Layer Meteorol.* **2**, 228–245.

Monin, A. S. and Yaglom, A. M.: 1971, 'Statistical Fluid Mechanics', Vol. 1, The MIT Press, 769 pp.

Obukhov, A. M.: 1946, 'Turbulence in an Atmosphere with a Non-Uniform Temperature', *Trudy Inst. Teoret. Geofiz. AN SSSR* (Works Inst. Theor. Geophys. Acad. Sci. USSR) **1**, 95–115 (English translation in *Boundary-Layer Meteorol.* 1971, **2**, 7–29).

Obukhov, A. M.: 1960, 'Structure of Temperature and Velocity Fields Under Conditions of Free Convection', *Izv. Akad. Nauk SSSR, Ser. Geofiz.* (Bull. Acad. Sci. USSR, Ser. Geophys.) No. 9, 1392–1396.

Prandtl, L.: 1932, 'Meteorologische Anwendungen der Strömungslehre', *Beitr. Phys. f. Atmosph.* **19**, 188–202.

Priestley, C. H. B.: 1959, 'Turbulent Transfer in the Lower Atmosphere', Chicago Univ. Press.

Pruitt, W. O., Morgan, D. L., and Lourence, F. J.: 1973, 'Momentum and Mass Transfers in the Surface Boundary Layer', *Quart. J. Roy. Meteorol. Soc.* **99**, 370–386.

Skeib, G.: 1980, 'Zur Definition universeller Funktionen für die Gradienten von Windgeschwindigkeit und Temperatur in der Bodennahen Luftschicht', *Z. Meteorol.* **30**, 23–32.

Tsvang, L. R., Koprov, B. M., Zubkovskii, S. L., Dyer, A. J., Hicks, B., Miyake, M., Stewart, R. W., and McDonald, J. W.: 1973, 'A Comparison of Turbulence Measurements by Different Instruments; Tsimlyansk Field Experiment 1970', *Boundary-Layer Meteorol.* **3**, 499–521.

Webb, E. K.: 1958, 'Vanishing Potential Temperature Gradients in Strong Convection', *Quart. J. Roy. Meteorol. Soc.* **84**, 118–125.

Webb, E. K.: 1982, 'Profile Relationships in the Superadiabatic Surface Layer', *Quart. J. Roy. Meteorol. Soc.* **108**, 661–668.

Yaglom, A. M.: 1977, 'Comments on Wind and Temperature Flux-Profile Relationships', *Boundary-Layer Meteorol.* **11**, 89–102.

Zilitinkevich, S. S.: 1971, 'Turbulence and Diffusion under Conditions of Free Convection', *Izv. Akad. Nauk SSSR, Fiz. Atm. i Okeana* (Bull. Acad. Sci. USSR, Atmospheric and Oceanic Physics) **7**, 1263–1269.

Zilitinkevich, S. S. and Chalikov, D. V.: 1968, 'On the Determination of the Universal Wind and Temperature Profiles in the Surface Layer of the Atmosphere', *Izv. Akad. Nauk SSSR, Fiz. Atm. i Okeana* (Bull. Acad. Sci. USSR, Atmospheric and Oceanic Physics) **4**, 294–302.